



Discharge behavior of Mg–4 wt%Ga–2 wt%Hg alloy as anode for seawater activated battery

Jun Zhao, Kun Yu*, Yanan Hu, Shaojun Li, Xin Tan, Fuwen Chen, Zhiming Yu

School of Materials Science and Engineering, Central South University, Changsha 410083, China

ARTICLE INFO

Article history:

Received 7 March 2011

Received in revised form 21 June 2011

Accepted 21 June 2011

Available online 30 June 2011

Key words:

Mg–Ga–Hg alloy

Electrochemistry

Discharge behavior

Intermetallics

Seawater activated battery

ABSTRACT

Magnesium–gallium–mercury alloy is one of the new developed anode materials for seawater activated batteries. The potentiodynamic polarization, galvanostatic discharge and electrochemical impedance spectroscopy of Mg–4%Ga–2%Hg alloy in seawater are studied and compared with commercial AZ31 and AP65 alloys in this study. The results show that Mg–4%Ga–2%Hg alloy exhibits different discharge behaviors in as-cast, homogenizing, rolling and annealing conditions. The annealing Mg–4%Ga–2%Hg sheet obtains the most negative corrosion potentials in different current densities. And the Mg–4%Ga–2%Hg alloy provides more negative corrosion potentials than AZ31 and AP65 alloys. EIS studies reveal that the Mg–Ga–Hg alloy/seawater interfacial process is determined by an activation-controlled reaction. The Mg₃Hg and Mg₂₁Ga₅Hg₃ phases improve the electrochemical properties of Mg–4%Ga–2%Hg alloy. The assembled prototype battery with Mg–4%Ga–2%Hg alloy as anode and CuCl as cathodes exhibits a satisfactory discharge performance because of the advantages in discharge characterizations and microstructure of the Mg–4%Ga–2%Hg alloy.

© 2011 Elsevier Ltd. All rights reserved.

1. Introduction

Seawater activated batteries are potential power sources for underwater instruments such as sonobuoys, underwater defense devices, air–sea rescue equipment and meteorological radiosondes [1]. Such batteries can be designed for a wide range of duty cycles, from a few minutes to several days, for low and high current, pulsed and constant operation [2]. Because seawater is the electrolyte, the electrodes are not housed in a pressure case and the power density is potentially very high [3]. Such advantages provide higher practicability and lower cost for seawater activated batteries than lithium or alkaline batteries for subaqueous applications. The seawater activated batteries rely on the corrosion of a reactive metal anode in seawater and the reduction of oxygen or water at an inert cathode to generate an electrochemical potential [3]. Hence, the key material applied in the seawater batteries is the metal anode, which increases the cell voltages and minimizes self-discharge [4]. Magnesium offers several advantages as an anode material in such battery, for example a high electrode potential of -2.73 V vs. normal hydrogen electrode (NHE), a high faradic capacity, appropriate corrosion rate and low density [5]. In the past few years, several seawater activated magnesium alloy anodes have been developed

for military and commercial applications but many designs are apparently unpublished or patented [6–8]. The electrochemical characterizations of reported commercial magnesium alloys show that the typical anode materials for seawater activated batteries were Mg–Al system alloys, including AZ31 (Mg–3%Al–1%Zn), AZ61 (Mg–6%Al–1%Zn) and AP65 (Mg–6%Al–5%Pb) alloys [6,9]. But the previous investigations show that AZ31 and AZ61 alloys are unsuitable to be used as the battery anodes in seawater system or even including Mg(ClO₄)₂, MgBr₂ and MgCl₂ electrolyte solution systems because they cannot provide enough cell voltages [10]. Only AP65 alloy can be used in some seawater activated battery because it provides high corrosion potential. It can be assembled with cuprous chloride (CuCl) or silver chloride (AgCl) to fabricate seawater activated batteries [11]. But the specific energy of the battery using AP65 alloy anode is not high enough to be used in many instruments which need high power over 100 W h Kg⁻¹ [12]. One of the new developed magnesium alloys used as seawater activated battery anode is magnesium–gallium–mercury system alloy because it can provide a high specific energy of about 150 W h Kg⁻¹ in the battery. Mercury is an effective element used in the metal anode materials to improve the corrosion voltage. Gallium is an element to control the corrosion behaviors of metal anode and provide a high specific energy of the battery [13]. Furthermore, Mg–Ga–Hg alloy anode can even be used as a semi-fuel cell as well as a battery. Up to now, there are few reports about the Mg–Ga–Hg alloy, which used seawater activated battery anode materials. Thus, in

* Corresponding author. Tel.: +86 731 88879341, fax: +86 731 88876692.
E-mail address: yukungroup@gmail.com (K. Yu).

order to achieve good performance of Mg–Ga–Hg alloy anode, it is necessary to obtain a thorough understanding of the associated electrochemical discharge behavior of Mg–Ga–Hg alloy. Accordingly, the present study examines the discharge behaviors of a Mg–4%Ga–2%Hg (wt%) alloy in the artificial seawater, and compares its electrochemical properties with those of AP65 and AZ31 alloy. The relationship between various discharge parameters and microstructure of Mg–4%Ga–2%Hg alloy in as-cast, homogenizing, rolling and annealing states are also discussed. And a simple prototype battery is assembled with Mg–4%Ga–2%Hg alloy sheet as anode and CuCl as cathode to evaluate its discharge properties in seawater.

2. Material and method

The Mg–4%Ga–2%Hg (wt%) alloy was melted with high purity magnesium (>99.9%), gallium (>99.99%) and mercury (>99.99%). The analyzed chemical composition of the experimental alloy was Mg–4.13%Ga–2.21%Hg (impurity Si < 0.05%, Fe < 0.01%, Cu < 0.005%, Ni < 0.005%, Ca < 0.005%). The experimental Mg–4%Ga–2%Hg alloy melted at 953 K with a protection of a special flux and Ar₂ + SF₆ gas mixture to impede the reduction of gallium or mercury at high temperature. The molten alloy was casted in the water-cooled copper mold. Then the as-cast Mg–Ga–Hg alloy ingot was homogenized at 698 K for 16 h and hot rolled to sheets with 0.4 mm in thickness with several rolling passes. During every hot rolling passes, the experimental alloy plates were reheated to 673 K for 0.5 h to improve the deformability. At last, the rolled Mg–4%Ga–2%Hg alloy sheets were annealed at 533 K for 2 h. Different specimens in as-cast, homogenizing, rolling and annealing conditions were prepared for the electrochemical testing to investigate the discharge behaviors of Mg–4%Ga–2%Hg alloy.

All the specimens used for the electrochemical testing were polished with 1000 grit SiC emery paper and exposed to test with a surface of 10 mm × 10 mm. The Solartron SI 1287 potentiostat/galvanostat system was used in a three-electrode configuration for testing the half-cell characterization of the experimental alloys. The working electrode was the experimental Mg–4%Ga–2%Hg alloy and the counter electrode was a Platinum plate. A saturated calomel electrode (SCE) served as the reference electrode and all potentials are reported with respect to such reference electrode in this study except for special illustration. The polarization, galvanostatic test and electrochemical impedance spectroscopy (EIS) of Mg–4%Ga–2%Hg alloy anode were measured and the data were acquired and processed by the Zplot/Zview software version 2.6. Three samples in different conditions were tested for the electrochemical properties and the minimum values were reported. And the discharge behaviors of experimental Mg–4%Ga–2%Hg alloy were compared with AZ31 and AP65 alloy sheets from Magnesium Elektron UK under three electric current densities 10 mA cm⁻², 100 mA cm⁻² and 200 mA cm⁻² respectively. At last, the prototype battery with ten pieces of Mg–4%Ga–2%Hg alloy sheets as anode and CuCl as cathode was assembled and discharged in seawater.

The electrolyte in this study was artificial seawater with a pH 7.02. Its composition is 26.5 g l⁻¹ NaCl + 24 g l⁻¹ MgCl₂ + 0.73 g l⁻¹ KCl + 3.3 g l⁻¹ MgSO₄ + 0.2 g l⁻¹ NaHCO₃ + 1.1 g l⁻¹ CaCl₂ + 0.28 g l⁻¹ NaBr [14]. The temperature of the artificial seawater in this study is 286 ± 1 K.

The microstructure and the surface morphology of the experimental Mg–4%Ga–2%Hg alloy in different conditions were observed by using a Polyvar-MET metallographic microscope, a JSM-5600Lv scanning electron microscopy (SEM) with Energy-dispersive X-ray spectroscopy (EDS).

3. Results and discussion

3.1. Microstructures of Mg–4%Ga–2%Hg alloy in different conditions

Since the microstructures of Mg–4%Ga–2%Hg alloy in as-cast, homogenizing, hot rolling and annealing conditions play important effects on its discharge behaviors in the sequent electrochemical experiment, the observation of microstructural morphology and the identification of intermetallics are performed first to analyze the relationship between the microstructure and the electrochemical properties. The microstructures of experimental Mg–4%Ga–2%Hg alloy in different conditions are shown in Fig. 1. It shows dendritic structure morphology with many coarse intermetallics both on the grain boundary and in the matrix in as-cast state (Fig. 1a). Obviously, the morphology, size, and distribution of such intermetallics influence the electrochemical characterization of Mg–4%Ga–2%Hg alloy because of their cathodic qualities in the corrosion galvanic cell. After the homogenizing of the as-cast Mg–4%Ga–2%Hg alloy, it can be observed two distinct shape intermetallics in the microstructure. One is large with a block shape, and the other is dispersed point shape (Fig. 1b). With a composition analysis of EDS by using SEM (Fig. 1c and d) and the XRD phase identification (Fig. 1e), it is found that the block shape intermetallic is Mg₃Hg. And the dispersed point shape phase is Mg₂₁Ga₅Hg₃. The solid solubility of Hg in α-Mg matrix is so limited (<0.1 at%) that it is hard for Mg₃Hg phase to dissolve in the α-Mg even homogenized at 698 K for 16 h. Hence, the Mg₃Hg phase maintains the block shape similar to its morphology in the as-cast state. But the Mg₂₁Ga₅Hg₃ phase can dissolve in the α-Mg matrix to form solid solution because the solubility of such intermetallic in α-Mg is over 3 at% at 695.7 K. And the dispersed Mg₂₁Ga₅Hg₃ phase probably precipitates from the solid solution of α-Mg matrix during the slow cooling process of homogenization. As a result, the heat treatment of as-cast Mg–4%Ga–2%Hg specimen can homogenize the composition of alloy and modify the morphology of the Mg₂₁Ga₅Hg₃ phase. The intermetallics in the hot rolled Mg–4%Ga–2%Hg alloy sheet disperse along the rolling direction (Fig. 2a). Especially, the block shape intermetallic Mg₃Hg phase is broken up to small spot shape and distributes more uniformly. After the annealing treatment of rolled experimental alloy, all intermetallics in the Mg–4%Ga–2%Hg sheet distribute homogeneously (Fig. 2b) and the sheet can be treated as the anode material to be assembled in the seawater activated batteries.

3.2. Discharge behaviors of Mg–4%Ga–2%Hg alloy in different conditions

The potentiodynamic polarization behaviors of the Mg–4%Ga–2%Hg alloy in different conditions are shown in Fig. 3. The polarization parameters measured from the polarization curves are given in Table 1. The results show apparent variations in the corrosion potential and the corrosion current density of Mg–4%Ga–2%Hg alloy in different conditions. In hot rolling and annealing conditions, the corrosion potentials of experimental alloy are more negative than those of alloy in

Table 1
Parameters of Mg–4%Ga–2%Hg alloy from Polarization curves.

Condition	Corrosion potential (V)	Corrosion current <i>I</i> _{corr} (A cm ⁻²)
As-cast	–1.5471	2.0142 × 10 ⁻⁴
Homogenization	–1.6007	2.7034 × 10 ⁻⁴
Rolling	–1.7394	4.2884 × 10 ⁻⁴
Annealing	–1.7606	4.5347 × 10 ⁻⁴

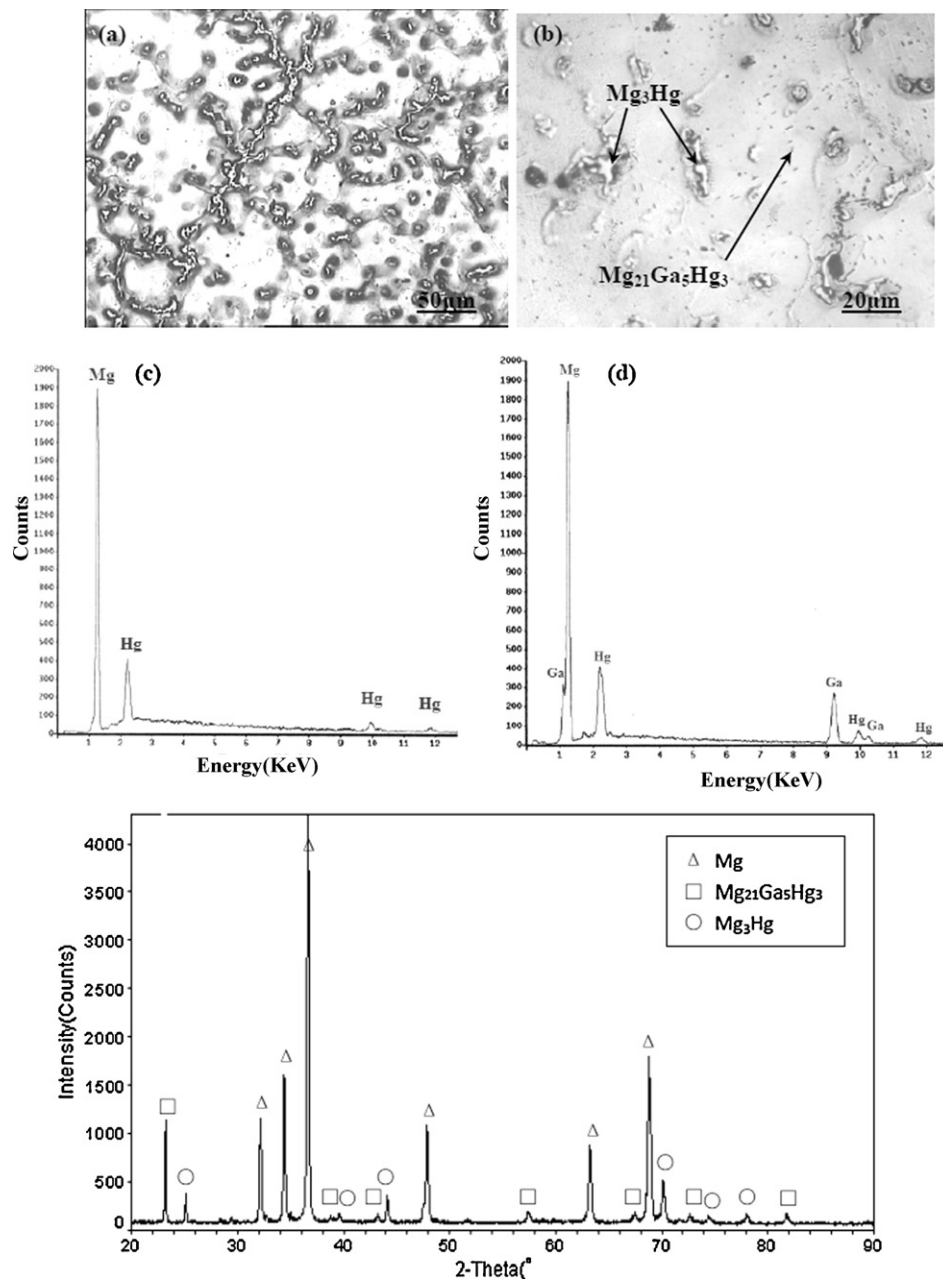


Fig. 1. Microstructures and phase identification of Mg-4%Ga-2%Hg alloy in different conditions. (a) Morphology of Mg-4%Ga-2%Hg alloy in as-cast state; (b) morphology of intermetallics in homogenized state; (c) EDS identification of Mg₃Hg phase; (d) EDS identification of Mg₂₁Ga₅Hg₃ phase; (e) XRD phase identification of Mg-4%Ga-2%Hg alloy.

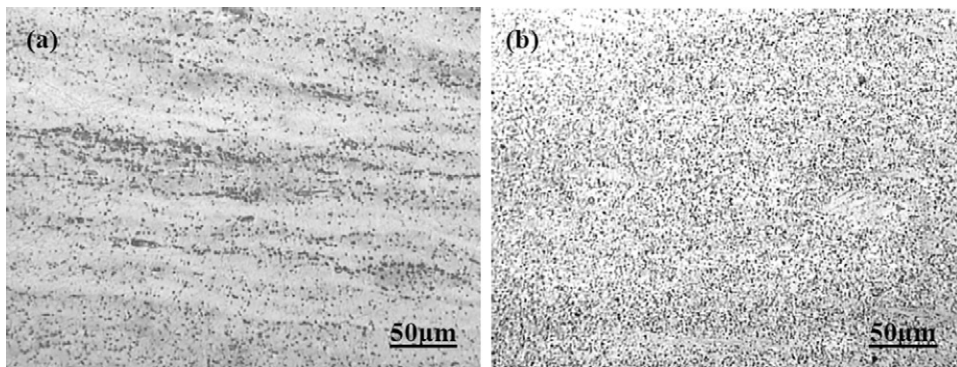


Fig. 2. Morphology of hot rolled and annealed Mg-4%Ga-2%Hg alloy sheet. (a) Morphology of hot rolled Mg-4%Ga-2%Hg alloy sheet; (b) morphology of annealed Mg-4%Ga-2%Hg alloy sheet.

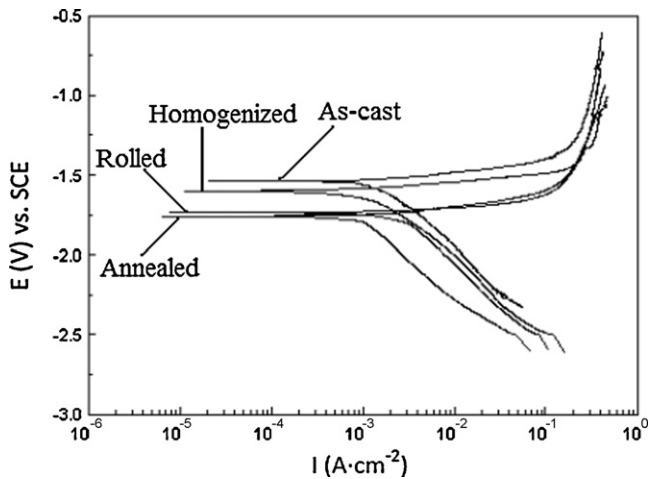


Fig. 3. Potentiodynamic polarisation behavior of Mg-4%Ga-2%Hg alloy in different conditions.

as-cast and homogenization states. The corrosion potential shifts negatively by 0.2135 V, meanwhile the corrosion current increases by $2.5205 \times 10^{-4} \text{ A cm}^{-2}$. Although the standard potential of the magnesium electrode is -2.73 V (vs. NHE), the steady-state working potential is generally about -1.50 V (vs. NHE). This deviation in potential is due to the formation of a magnesium hydroxide film on the metal surface. Therefore, the more negative corrosion potential with higher corrosion current is benefit for the utilization of Mg-Ga-Hg alloy as anode in the seawater activated battery. The electrochemical reactions for Mg alloy anode seawater battery can be described as the following reaction mechanism [15]:



Therefore, the anode will undergo hydrogen evolving corrosion:



The discharge reaction can be minimized by the corrosion product Mg(OH)_2 which pastes on the surface of Mg-4%Ga-2%Hg alloy and results in the reducing of anode reacting area. But the dispersed distribution of intermetallic $\text{Mg}_{21}\text{Ga}_5\text{Hg}_3$ and Mg_3Hg phases in the α -Mg matrix makes the electrochemical reactions more uniform and increases the corrosion rate. Such is benefit to the

continuation and stable discharge reaction of the Mg-4%Ga-2%Hg anode alloy. This phenomenon can be observed on the corrosion surface of the specimens after discharging as shown in Fig. 4. Fig. 4a shows that the corrosion products around the $\text{Mg}_{21}\text{Ga}_5\text{Hg}_3$ phase (white point phase with EDX analysis in Fig. 4b) break off and result in the corrosion reaction penetrate into the interior of Mg-Ga-Hg alloy matrix. And such continuous corrosion provides the more negative discharge potential from -1.5471 V to -1.7606 V for annealed Mg-4%Ga-2%Hg anode alloy than ordinary magnesium alloy. This corrosion process can be illustrated by the schematic diagram as shown in Fig. 5a. The corrosion of α -Mg matrix around the $\text{Mg}_{21}\text{Ga}_5\text{Hg}_3$ phase is serious than other place and the corrosion products can be removed from the surface of alloy. Mg(OH)_2 is the main solid corrosion products produced by the reaction (3). Mg(OH)_2 can impede the corrosion penetrate into the Mg Matrix. But the high concentration of chloride ions in seawater can accelerate the corrosion rate by transforming the formed Mg(OH)_2 into more soluble MgCl_2 . The breakdown of Mg(OH)_2 layer decreases the protected area on the surface of specimen, consequently promoting further dissolution of the substrate. The chloride ions are involved in the α -Mg matrix dissolution by accelerating the electrochemical reaction from magnesium to magnesium univalent ions. So, the surface morphology of specimen becomes a rimous view as shown in Fig. 5b. Such unprotected surface is beneficial to maintain continuous corrosion reaction and provide stable discharge potential of the Mg-Ga-Hg alloy anode. Hence, the galvanostatic discharge behaviors of Mg-4%Ga-2%Hg alloy in different conditions are measured and shown in Fig. 6. Three different electric current densities (1 mA cm^{-2} , 150 mA cm^{-2} and 300 mA cm^{-2}) are performed to evaluate the variation of corrosion potentials. The electrochemical parameters are listed in Table 2. Based on the galvanostatic measurement test, it can be seen that there is little difference between Mg-4%Ga-2%Hg in different conditions at a very low current density of 1 mA cm^{-2} . With the increasing of discharge current density, the corrosion potentials in different conditions of Mg-4%Ga-2%Hg alloy become more and more different. The discharge voltage values in as-cast and homogenization state are -1.2453 V to $\sim -1.4338 \text{ V}$ at 150 mA cm^{-2} and -0.9452 V to $\sim -1.1136 \text{ V}$ at 300 mA cm^{-2} . Such results confirm that Mg-4%Ga-2%Hg alloy in as-cast and homogenization states only provide relative low discharge voltage values which hardly meet the application requirements as a seawater activated battery anode. The Mg-4%Ga-2%Hg alloy obtains the most negative discharge

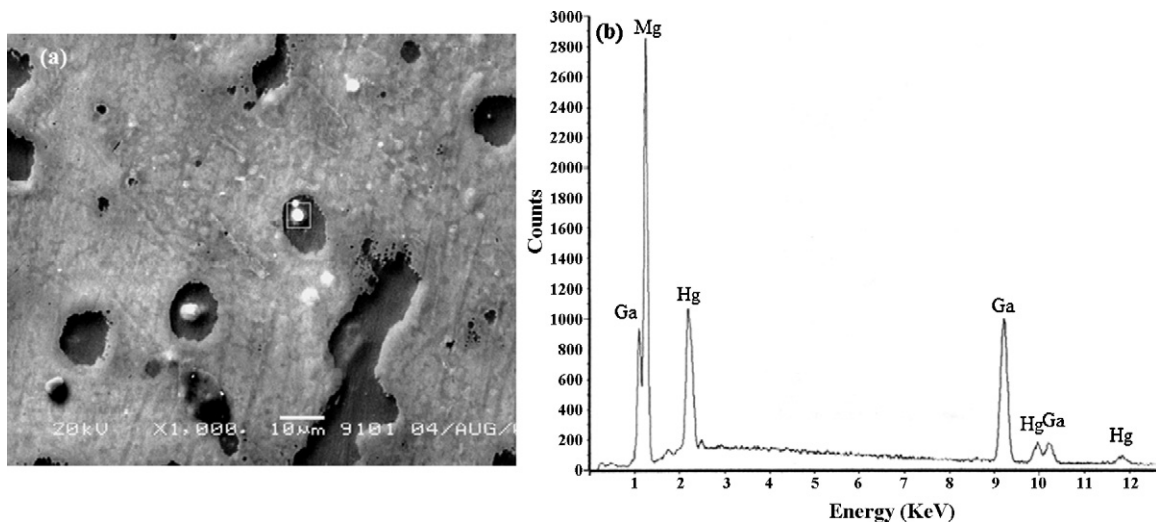


Fig. 4. Morphology and phase identification of Mg-4%Ga-2%Hg alloy after discharging. Corrosion surface morphology of Mg-4%Ga-2%Hg alloy; EDS identification of $\text{Mg}_{21}\text{Ga}_5\text{Hg}_3$ phase after discharging.

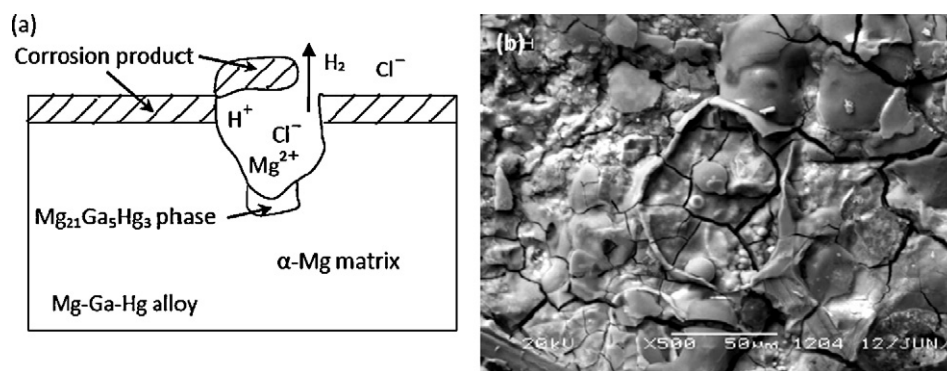


Fig. 5. Schematic diagram and corrosion products of Mg-4%Ga-2%Hg alloy after discharging. Corrosion schematic diagram of Mg-4%Ga-2%Hg alloy SEM image of corrosion surface and products of Mg-4%Ga-2%Hg alloy.

Table 2

Galvanostatic discharge parameters of Mg-4%Ga-2%Hg alloy in different conditions.

Alloy	1 mA cm ⁻²		150 mA cm ⁻²		300 mA cm ⁻²	
	Open circuit voltage (V)	Average voltage (V)	Open circuit voltage (V)	Average voltage (V)	Open circuit voltage (V)	Average voltage (V)
As-cast	-1.9856	-1.9601	-1.8605	-1.2453	-1.9139	-0.9452
Homogenization	-1.9881	-1.9677	-1.9729	-1.4338	-1.9321	-1.1136
Rolling	-1.9851	-1.9702	-1.9619	-1.6008	-1.9579	-1.1917
Annealing	-1.9924	-1.9714	-1.9681	-1.6304	-1.9469	-1.2149

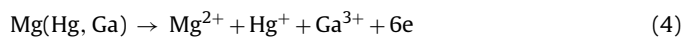
voltage value in annealing state with different electric current densities. Especially it provides an average -1.6304 V with the electric current density of 150 mA cm^{-2} . Such high voltage value indicates the annealed Mg-4%Ga-2%Hg alloy sheet has the potential to provide a higher specific energy if it is assembled in a cell battery. The annealed Mg-4%Ga-2%Hg alloy also gets a very short activation time with only a few seconds at the beginning stage of discharge process. Such property is necessary for Mg-Ga-Hg alloy to act as a battery anode in practical applications.

3.3. Discharge behavior of Mg-4%Ga-2%Hg alloy compared with AZ31 and AP65 Mg alloys

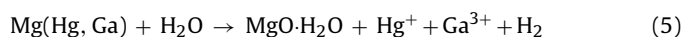
For further understanding the discharge behaviors of Mg-4%Ga-2%Hg alloy compared with other commercial magnesium alloy anode materials, the galvanostatic measurements of annealed Mg-4%Ga-2%Hg alloy sheets with AZ31 and AP65 alloy sheets are performed with three different current densities 10, 100 and 200 mA cm^{-2} respectively as shown in Fig. 7. The detail discharge parameters are listed in Table 3. The low current density of 10 mA cm^{-2} aims to evaluate the discharge behavior of power source anode material for long-term low-power applications. And the higher current densities, such as 100 and 200 mA cm^{-2} , are used to measure the discharge behavior of anode for high-power applications. The results show that the corrosion potentials of AZ31 alloy are more positive than those of AP65 and Mg-4%Ga-2%Hg alloy. Such results confirm that AZ31 alloys can hardly be used as a seawater activated battery anode. The AP65 alloy can be used as battery anode material due to its high corrosion potential value during the discharge process. And the Mg-4%Ga-2%Hg alloy provides the most negative voltage values of all the alloys with different current densities, especially it provides an average -1.5937 V with high electric current density of 200 mA cm^{-2} .

Another obvious difference between the electrochemical characterizations of Mg-4%Ga-2%Hg alloy with AZ31 and AP65 alloys is the anodic polarization behavior during the discharge process. As shown in Fig. 6, the Mg-4%Ga-2%Hg alloy maintains a stable

corrosion potential value during the whole discharge process. But the corrosion potential values of AZ31 and AP65 alloys will first move to negative and then move to positive because of the polarization effect. This difference is due to the different compounds, which influence the corrosion behaviors in different alloys. The typical compounds, such as $\text{Mg}_{17}\text{Al}_{12}$ phase in AZ31 and AP65 alloy, will hinder the corrosion process during the discharge process and result in an obviously anodic polarization effect. But the Mg_3Hg and $\text{Mg}_{21}\text{Ga}_5\text{Hg}_3$ phases in Mg-4%Ga-2%Hg alloy obtain a great electrode potential difference between them with the α -Mg matrix. Such two compounds in Mg-4%Ga-2%Hg alloy will accelerate the corrosion of α -Mg matrix and induce the corrosion penetrate into the internal of alloy. The corrosion activation reaction can be described as:



or



The dissolving of α -Mg matrix with Mg_3Hg and $\text{Mg}_{21}\text{Ga}_5\text{Hg}_3$ will produce Hg and Ga ions, which combine with Mg to produce amalgam that react severely with water and maintain the activation reaction circle. Furthermore, the corrosion products on the surface of Mg-4%Ga-2%Hg alloy fall off easily and cannot paste sturdy enough to prevent the continue corrosion of the α -Mg matrix in the Cl^- environment of artificial seawater. All these reasons will result in a persistent corrosion and steady discharge potential of Mg-4%Ga-2%Hg alloy.

Since the use of an A.C. signal can provide more information than that obtained from D.C. polarization technique, the electrochemical impedance spectroscopy is used to study the discharge behavior and corrosion mechanism of Mg-4%Ga-2%Hg alloy in present investigation. Generally, the simple electrochemical system consists of a double-layer capacitance (C_{dl}), a solution resistance (R_s) and a charge-transfer resistance (R_{ct}) [9,16]. The impedance locus diagrams of Mg-4%Ga-2%Hg, AP65 and AZ31 alloys are obtained by applying a frequency range of 0.01–100 kHz with a AC amplitude of 10 mV. The Z/phase (θ) relation of the impedance is given by

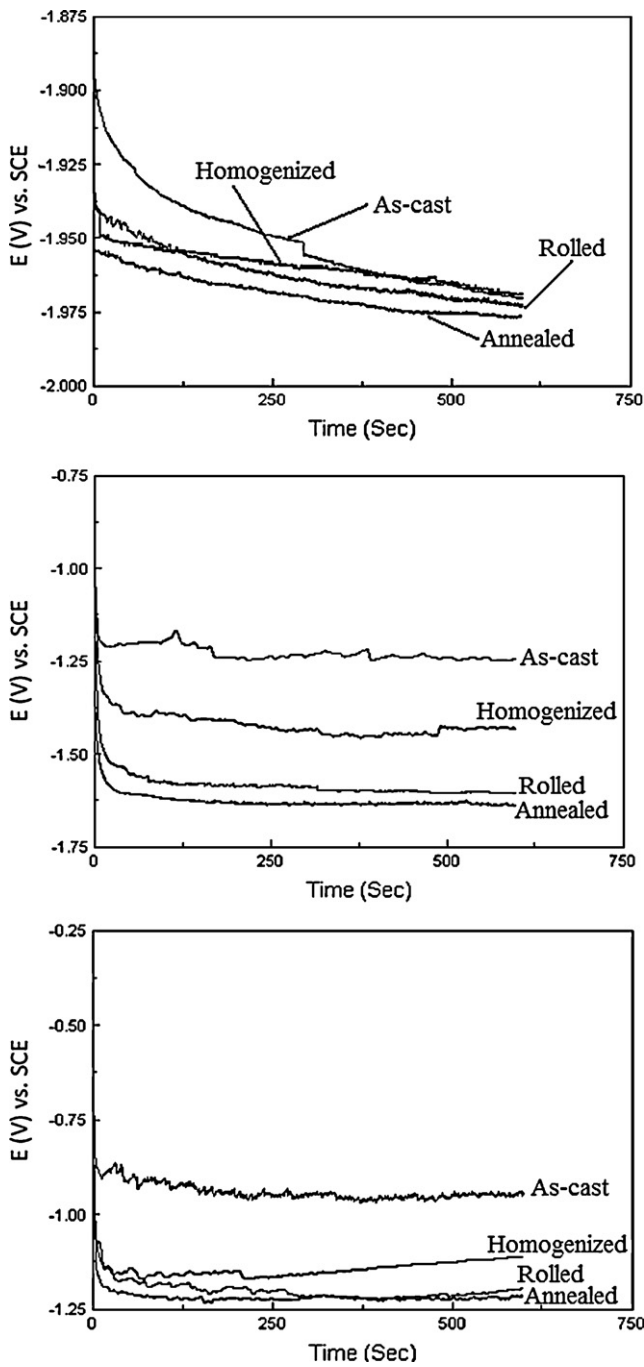


Fig. 6. Galvanostatic discharge behavior of the Mg-4%Ga-2%Hg alloy in different conditions. (a) Galvanostatic discharge behavior at 1 mA cm⁻², (b) galvanostatic discharge behavior at 150 mA cm⁻², (c) galvanostatic discharge behavior at 300 mA cm⁻².

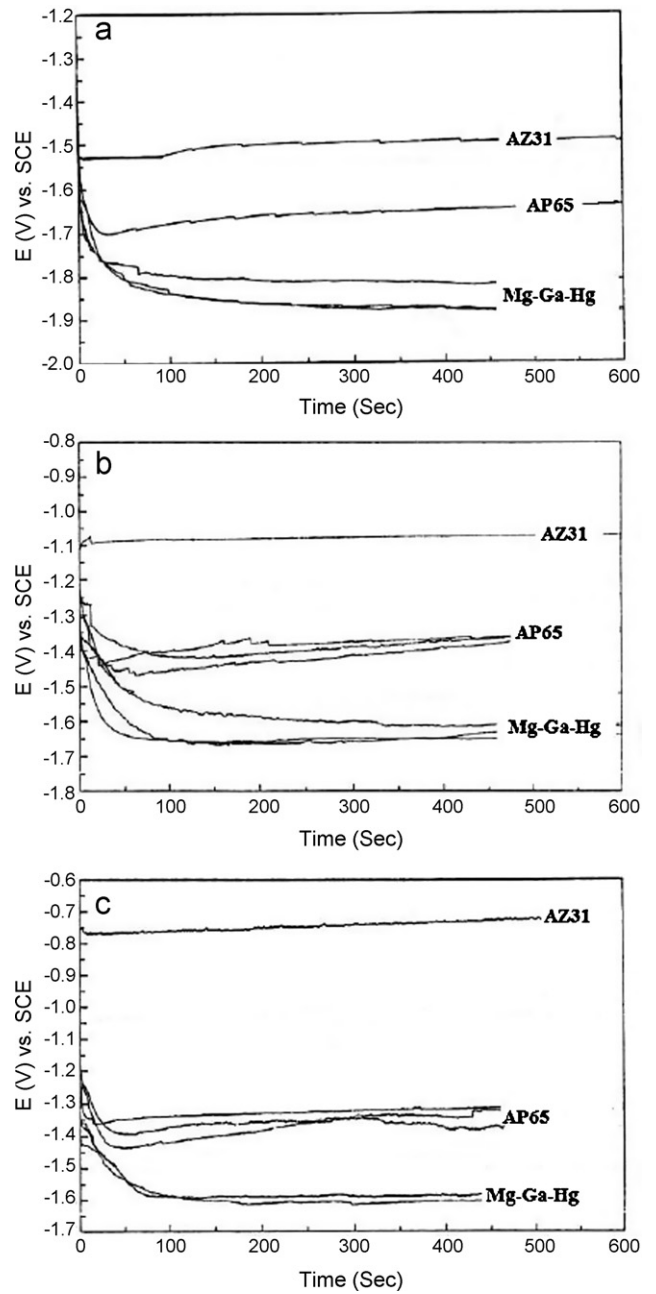


Fig. 7. Galvanostatic discharge behavior of Mg-4%Ga-2%Hg, AZ31 and AP65 alloys in different conditions. (a) Galvanostatic discharge behavior at 10 mA cm⁻², (b) galvanostatic discharge behavior at 100 mA cm⁻², (c) galvanostatic discharge behavior at 200 mA cm⁻².

$Z' = Z \cos(\theta)$ for the real part and $Z'' = Z \sin(\theta)$ for the imaginary part. Typical Nyquist plots for the three magnesium alloys are shown in Fig. 8a–c respectively. The Nyquist plot shows that the curves of three alloys have a single capacitive loop at all frequencies. The

Table 3
Galvanostatic discharge parameters of alloys in different conditions.

Alloy	10 mA cm ⁻²		100 mA cm ⁻²		200 mA cm ⁻²	
	Open circuit voltage (V)	Average voltage (V)	Open circuit voltage (V)	Average voltage (V)	Open circuit voltage (V)	Average voltage (V)
AZ31	-1.5451	-1.5034	-1.5437	-1.0254	-1.5532	-0.7252
AP65	-1.7560	-1.6587	-1.6869	-1.4848	-1.7261	-1.4041
Mg-4%Ga-2%Hg	-1.9232	-1.8714	-1.9118	-1.6378	-1.9193	-1.5973

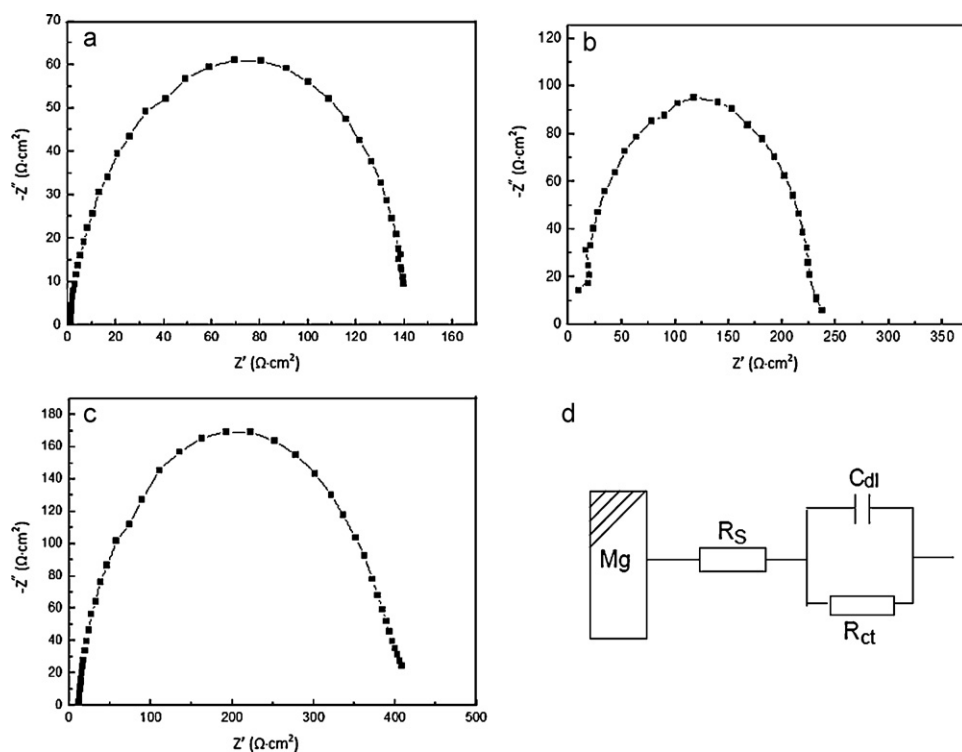


Fig. 8. Electrochemical impedance spectroscopy measurements of different magnesium alloys. (a) Nyquist plots for Mg–4%Ga–2%Hg alloy, (b) Nyquist plots for AP65 alloy, (c) Nyquist plots for AZ31 alloy, (d) the equivalent circuit of magnesium alloys in seawater.

nature of the curves indicates whether the system is activation-controlled (a semicircle), diffusion-controlled (a 45° straight line), or a combination of both [16]. In this experiment, semicircles have been obtained and this indicates that the electrode/electrolyte interface in this study is controlled predominantly by activation-controlled processes.

The diameter of the semicircle gives the charge-transfer resistance (R_{ct}) at the electrode/electrolyte interface, which relates to the corrosion rate. The intercept on the x -axis at the higher frequencies gives the solution resistance (R_s). In order to enable a detail analysis of the impedance diagram, the equivalent circuit model reported in Fig. 8d and the obtained parameters such as R_s , C_{dl} and R_{ct} are shown in Table 4. The EIS spectra of three alloys are similar except in diameter, which shows that the corrosion mechanism is same but the corrosion rate is different. The least diameter is obtained with Mg–4%Ga–2%Hg alloy indicates that the corrosion resistance of such alloy is the lowest. The corrosion rate is inversely related to R_{ct} . Higher the R_{ct} value, lower the corrosion rate. And the order of the R_{ct} values with respect to three experimental alloys is: AZ31 > AP65 > Mg–4%Ga–2%Hg, which reflects the corrosion rate of Mg–4%Ga–2%Hg alloy is the highest. The low C_{dl} value for the magnesium alloy implies the formation of relatively thick and compact protective film on the alloy surface. As expected, the Mg–4%Ga–2%Hg alloy obtains the highest C_{dl} value and AZ31 alloy obtained the lowest value. In the present study, it is also seen that increasing of R_{ct} is accomplished by the reduction of C_{dl} due to the total difference corrosion behaviors among these three alloys. In

general, the intermetallics in the alloy make great effects on the electrochemical corrosion behavior. During corrosion process, the $Mg_{17}Al_{12}$ phase in AZ31 alloy is highly stable and acts as effective barrier. Hence, the corrosion product film on such phase is continuous so that the dissolution of α -Mg is inhibited. The discharge process of AZ31 alloy will be impeded so that it cannot be used as the seawater activated anode. On the contrary, the Mg–4%Ga–2%Hg alloy cannot form effective protective film in chloride environment. The Mg_3Hg and $Mg_{21}Ga_5Hg_3$ phases in this alloy are activated easier and accelerate the corrosion of α -Mg matrix. The addition of Ga and Hg in the alloy promotes the electrochemical activity and let the anode reaction persistently. The Mg_3Hg phase and the amalgam produced by it during the electrochemical reactions provide enough negative potential for the application of battery. The solid solution of Ga in α -Mg and the dispersed distribution of $Mg_{21}Ga_5Hg_3$ phase which precipitates from the solid solution of α -Mg matrix produce a less charge-transfer resistance in the faradaic reaction, which leads to a good electrochemical performance such as the fast activity time and negative corrosion potential. Meanwhile, the dispersed and small size $Mg_{21}Ga_5Hg_3$ phase can adjust the corrosion current density and reduce the electro-negativity discrepancy between α -Mg matrix and Mg_3Hg phase. That leads to a controllable corrosion driving force and let the alloy exhibit an appropriate corrosion rate during the discharge process. Such results match with the electrochemical measurements of polarization and galvanostatic discharge behaviors.

3.4. Discharge properties of a prototype battery assembled by Mg–4%Ga–2%Hg alloy as anode

The simple prototype battery is assembled by ten pieces of Mg–4%Ga–2%Hg alloy sheets with a size of $450\text{ mm} \times 450\text{ mm} \times 0.4\text{ mm}$ as anode and cuprous chloride as cathodes. And the electrolyte is artificial seawater at $286 \pm 1\text{ K}$. The prototype battery activated by seawater had satisfactory

Table 4

Corrosion parameters obtain from EIS measurement for different alloys.

Alloy	R_s ($\Omega\text{ cm}^2$)	C_{dl} (F)	R_{ct} ($\Omega\text{ cm}^2$)
Mg–4%Ga–2%Hg	9.41	1.29×10^{-3}	138.7
AP65	8.87	8.48×10^{-4}	222.6
AZ31	7.39	1.33×10^{-5}	398.7

Table 5

Typical discharge properties of prototype battery.

Activation time (s)	Maximum voltage (V)	Average voltage of the entire discharge process (V)	Total discharge time (min)	Hydrogen emission rate ($\text{l cm}^{-2} \text{min}^{-1}$)	Specific energy (Wh kg^{-1})
5.7	1.451	1.393	25	$(0.37\text{--}0.49) \times 10^{-3}$	147

discharge properties as shown in Table 5. The activation time was measured as the time required by the battery to reach 70% of the maximum voltage. For the Mg–4%Ga–2%Hg alloy anode, the activation time was only 5.7 s. The total discharge time of the battery persists 25 min. The average voltage of the cell is 1.393 V and the maximum voltage is 1.451 V. The Hydrogen emission rate is a parameter to evaluate the corrosion process. The measured $0.37\text{--}0.49 \times 10^{-3} \text{ l cm}^{-2} \text{ min}^{-1}$ value is acceptable for the application in seawater activated battery. Especially, the specific energy of the simple prototype battery obtains the excellent 147 Wh kg^{-1} . Compared with the published data of 30 Wh kg^{-1} for lead acid battery or 88 Wh kg^{-1} for AP65/AgCl seawater activated battery [17,18], the discharge performance of Mg–4%Ga–2%Hg alloy are superior to many of them.

4. Conclusions

The Mg–4%Ga–2%Hg alloy exhibits different discharge behaviors in as-cast, homogenizing, rolling and annealing states. The discharge potentials show that annealing Mg–4%Ga–2%Hg alloy sheet obtains the most negative voltage value at different discharge current densities. And the Mg–4%Ga–2%Hg alloy provides more negative corrosion potentials than AZ31 and AP65 alloys. EIS studies reveal that the electrode/electrolyte interfacial process is determined by an activation-controlled reaction. The C_{dl} values which imply the formation of relatively protective film on the Mg alloy surface follow the following sequence: Mg–4%Ga–2%Hg > AP65 > AZ31. Hence, the corrosion rate of Mg–4%Ga–2%Hg alloy is the highest. The Mg_3Hg and $\text{Mg}_{21}\text{Ga}_5\text{Hg}_3$ phases play important roles in promoting the electrochemical properties of Mg–4%Ga–2%Hg alloy. The Mg_3Hg phase provides enough negative potential and accelerates the dissolution of $\alpha\text{-Mg}$ in the seawater during the electrochemical reactions. The $\text{Mg}_{21}\text{Ga}_5\text{Hg}_3$ phase produce a less charge-transfer resistance in the faradaic reaction and adjust the electro-negativity discrepancy between $\alpha\text{-Mg}$ matrix and Mg_3Hg phase. The assembled prototype battery with Mg–4%Ga–2%Hg alloy as anode and CuCl as cathodes exhibits a

satisfactory discharge performance because of the advantages in discharge behaviors and microstructures of the Mg–4%Ga–2%Hg alloy, which can be used as a candidate for seawater activated battery anode.

References

- [1] M. Shinohara, E. Arakib, M. Mochizukic, Practical application of a sea-water battery in deep-sea basin and its performance, *J. Power Sources* 187 (2009) 253.
- [2] W.S.D. Wilcock, P.C. Kauffman, Development of a seawater battery for deep-water applications, *J. Power Sources* 66 (1997) 71.
- [3] H. Qistein, L. Torleif, H. Erik, A long-range, autonomous underwater vehicle using magnesium fuel and oxygen from the sea, *J. Power Sources* 136 (2004) 232.
- [4] R. Udhayan, N. Muniyandi, P.B. Mathur, Studies on magnesium and its alloys in battery electrolytes, *Br. Corros. J.* 27 (1992) 68.
- [5] J.R. Davis, *Handbook of Materials for Medical Devices*, ASM international, OH, 2006.
- [6] H. Zhao, P. Bian, D. Ju, Electrochemical performance of magnesium alloy and its application on the sea water battery, *J. Environ. Sci.* 21 (2009) S88.
- [7] <http://www.magnesium-elektron.com/products-services.asp?ID=12>.
- [8] R.K. Venkatesara, performance evaluation of Mg–AgCl batteries for under water propulsion, *Defense Sci. J.* 5 (2001) 161.
- [9] R. Udhayan, D.P. Bhatt, On the corrosion behaviour of magnesium and its alloys using electrochemical techniques, *J. Power Sources* 63 (1996) 103.
- [10] R. Thirunakaran, S. Vasudevan, A. Sivashanmugam, G. Kumar, N. Muniyandi, 1-Nitronaphthalene as a cathode material for magnesium reserve batteries, *J. Power Sources* 58 (1996) 213.
- [11] R. Renuka, AgCl and Ag₂S as additives to CuI in Mg–CuI seawater activated batteries, *J. Appl. Electrochem.* 27 (1997) 1394.
- [12] A. Pardo, M.C. Merino, A.E. Coy, R. Arrabal, F. Viejo, F. Matykina, Corrosion behaviour of magnesium/aluminium alloys in 3.5 wt%NaCl, *Corros. Sci.* 50 (2008) 823.
- [13] Y. Feng, R.C. Wang, K. Yu, C.Q. Peng, W.X. Li, Influence of Ga and Hg on microstructure and electrochemical corrosion behavior of Mg alloy anode materials, *Trans. Nonferrous Met. Soc. China* 17 (2007) 1363.
- [14] <http://en.wikipedia.org/wiki/Seawater>.
- [15] L.J. Liu, M. Schlesinger, Corrosion of magnesium and its alloys, *Corros. Sci.* 15 (2009) 1733.
- [16] G.L. Makar, J. Kruger, Corrosion of magnesium, *Int. Mater. Rev.* 38 (1993) 138.
- [17] S.S. Fira, K.B. Lee, L.W. Lin, Water-activated disposable and long shelf-life micro-batteries, *Sens. Actuators A* 111 (2004) 79.
- [18] J.G. Kim, J.H. Joo, S.J. Koo, Development of high-driving potential and high efficiency Mg-based sacrificial anodes for cathodic protection, *J. Mater. Sci. Lett.* 19 (2000) 477.